Received: 5 June 2023 | Revised: 3 August 2023 | Accepted: 9 August 2023

DOI: 10.1111/ppl.13999

ORIGINAL RESEARCH

Physiologia Plantarum

Biophysical and molecular characteristics of senescing leaves of two Norway maple varieties differing in anthocyanin content

Marjaana Rantala | Paula Mulo | Esa Tyystjärvi | Heta Mattila

Molecular Plant Biology, University of Turku, Turku, Finland

Correspondence
Heta Mattila, Molecular Plant Biology, University of Turku, Turku, Finland.
Email: h.mattila@ua.pt

Present address
Heta Mattila, Centre for Environmental and Marine Studies, University of Aveiro, Aveiro, Portugal.

Funding information
Academy of Finland, Grant/Award Numbers: 321616, 333421; The Ella and Georg Ehrnrooth Foundation; The Oskari Huttunen Foundation

Edited by A. Krieger-Liszkay

Abstract

Disassembly and degradation of the photosynthetic protein complexes during autumn senescence, a vital step to ensure efficient nutrient relocalization for winter storage, is poorly understood. Concomitantly with the degradation, anthocyanins are often synthesized. However, as to why leaves accumulate red pigments, no consensus exists. One possibility is that anthocyanins protect senescing leaves from excess light. In this study, we investigated the pigment composition, photosynthetic performance, radical production, and degradation of the photosynthetic protein complexes in Norway maple (*Acer platanoides*) and in its highly pigmented, purple-colored variety (Faassen's black) during autumn senescence, to dissect the possible roles of anthocyanins in photoprotection. Our findings show that senescing Faassen's black was indeed more resistant to Photosystem II (PSII) photoinhibition, presumably due to its high anthocyanin content, than the green maple. However, senescing Faassen's black exhibited low photosynthetic performance, probably due to a poor capacity to repair PSII. Furthermore, an analysis of photosynthetic protein complexes demonstrated that in both maple varieties, the supercomplexes consisting of PSII and its antenna were disassembled first, followed by the degradation of the PSII core, Photosystem I, Cytochrome b_6f, and ATP synthase. Strikingly, the degradation process appeared to proceed faster in Faassen's black, possibly explaining its poor PSII repair capacity. The results suggest that tolerance against PSII photoinhibition may not necessarily translate to a better fitness. Finally, thylakoids isolated from senescing and non-senescing leaves of both maple varieties accumulated very little carbon-centered radicals, suggesting that thylakoids may not be a major source of reactive oxygen species in senescing leaves.

1 | INTRODUCTION

Leaf senescence is a controlled process that comprises several phases in order to remobilize nutrients. To resorb the nutrients of the chlorophyll-binding protein complexes of the photosynthetic electron transport chain, Photosystem I (PSI) and Photosystem II (PSII) and their light-harvesting complexes (LHCI and LHCII, respectively), chlorophylls need to be detoxified into linear tetrapyrroles and stored in the vacuole of the senescing cell (Matile et al., 1988; for reviews, see Kuai et al., 2018; Wang & Grimm, 2021). Degradation of the protein

complexes follows chlorophyll degradation (Ito et al., 2022; Miersch et al., 2000; Nath et al., 2013; Tamary et al., 2019; Wang et al., 2014). The former has been studied mainly during developmental (age-related) senescence and at the level of individual protein subunits (for reviews, see Domínguez & Cejud, 2021; Krieger-Liszkay et al., 2019; Schöttler & Tóth, 2014). However, as the order in which the protein complexes are degraded varies between different species, even among different varieties of a species (Krupinska et al., 2012), and can be affected by weather conditions (Humbeck & Krupinska, 2003), the observations are difficult to generalize to other species and to other types of senescence.

During developmental senescence, preferential degradation of PSII often occurs (e.g., Nath et al., 2013) but early degradation of PSI has also been observed (Miersch et al., 2000; Wang et al., 2014). Usually, LHCs are degraded late and incompletely (e.g., Miersch et al., 2000), but this is not always the case (Krupinska et al., 2012). In addition, different LHC proteins can have different degradation rates (Moy et al., 2015; Nath et al., 2013).

Studies on the degradation of the photosystems during autumn senescence of deciduous species, on the other hand, are less common. Moy et al. (2015) reported that PSI is degraded before PSII in sugar maple (*Acer saccharum*) and swamp white oak (*Quercus bicolor*). Degradation of LHCs started at the same time as the degradation of the photosystems, although, in sugar maple, LHCII proteins were retained even at the end of senescence. In sugar maple, the amount of the PsbS protein decreased, while the PsbS amount strongly increased when the degradation of PSII was initiated in swamp white oak, and then again decreased toward the end of the senescence (Moy et al., 2015). In another study, probably conducted in senescing sycamore maple (*Acer pseudoplatanus*) although described as Norway maple (*Acer platanoides*), LHCII was observed to be degraded after PSII (Lepeduš et al., 2010). In the study of Lepeduš et al. (2010), PSII amount was measured via the D1 protein whose concentration may vary also due to photoinhibition of PSII (Theis & Schroda, 2016; Tyystjärvi, 2013; see below).

To our knowledge, the fates of cytochrome b_6f (Cyt b_6f) or ATP synthase (ATPase) are not known at the protein level during autumn senescence. In age-related senescence, Cyt b_6f is often reported to be one of the earliest complexes degraded, while ATPase is usually more stable (e.g., Domínguez & Cejud, 2021; Guiamét et al., 2002; Nath et al., 2013; Tamary et al., 2019; Wang et al., 2014). During age-related senescence, Rubisco is reported to be preferentially degraded (e.g., Nath et al., 2013). However, contrasting results have been obtained from deciduous trees (Lepeduš et al., 2008; Lepeduš et al., 2010; Millard & Thomson, 1989).

During autumn senescence, flavonoids may be synthetized (Lee et al., 2003; Mattila et al., 2018). Yellow autumn colors are mainly due to a slower degradation of carotenoids than chlorophylls, but red colors are caused by anthocyanin synthesis (Davies et al., 2022; Lee et al., 2003). Reasons behind the autumnal accumulation of red pigments have recently produced lively debates (e.g., Agati et al., 2021; Hughes et al., 2022; Lev-Yadun, 2022; Mattila & Tyystjärvi, 2023; Pena-Novas & Archetti, 2021; Renner & Zohner, 2022). The main hypotheses (which are not mutually exclusive) state that anthocyanins either protect senescing leaves from excess light or are involved in plants' defense against herbivores and/or pathogens.

In principle, anthocyanins could protect (senescing) leaves by shielding excess light (Field et al., 2001) or by scavenging reactive oxygen species, such as hydrogen peroxide (e.g., Gould et al., 2002; Kytridis & Manetas, 2006). Photoprotection can be estimated by measuring nutrient resorption (presumably a driver of evolution for features of autumn senescence; Duan et al., 2014; Field et al., 2001; Hoch et al., 2003), photosynthesis (e.g., carbon fixation; Lo Piccolo et al., 2018) or PSII functionality (Field et al., 2001; and many others). Light damages PSII with a rate that is directly proportional to the intensity of light (Tyystjärvi & Aro, 1996; for the mechanism(s), see Tyystjärvi, 2013; Mattila et al., 2023). Here, this irreversible light-induced damage to PSII is referred to as photoinhibition of PSII. To restore PSII activity, a new D1 protein (a core protein of PSII) has to be synthetized by the concurrent PSII repair cycle (for a review, see Theis & Schroda, 2016). Anthocyanins absorb green light efficiently; however, green light causes only little damage to PSII, at least in senescing leaves of Norway maple (Mattila & Tyystjärvi, 2023). Therefore, the fact that many anthocyanins also absorb blue light (e.g., Ji et al., 1992; for a review, see Landi et al., 2021) should contribute to their photoprotective capacity. Anthocyanin accumulation has been sometimes (Field et al., 2001; Hoch et al., 2003), but not always (Lo Piccolo et al., 2018; Mattila & Tyystjärvi, 2023), found to protect senescing autumn leaves.

Previously, we observed that the red sections of senescing leaves of Norway maple show more severe stress symptoms than the yellow sections (Mattila & Tyystjärvi, 2023; see also Nikiforou et al., 2011). In accordance, partially dead Norway maple trees show a higher frequency of red leaves than healthy trees (Sinkkonen, 2008). We proposed that if translocation of photosynthates is limited under adverse conditions, anthocyanins function as an additional electron sink, which helps photosynthesis to function and, thus, enables efficient nutrient resorption (Mattila & Tyystjärvi, 2023; for related suggestions, see Adams III et al., 2018; Hernandez & Van Breusegem, 2010; Lihavainen et al., 2021; Lo Piccolo et al., 2018; Soubeyrand et al., 2018). In addition, anthocyanin accumulation may be a response to nitrogen limitation, also in senescing trees (Hughes et al., 2022; Renner & Zohner, 2022).

Senescing Norway maple often contains both red and yellow leaves. On the other hand, a variety of Norway maple, Faassen's black, has heavily pigmented leaves, sometimes appearing almost black, already before autumn senescence (see Figure S1). In the present study, we used these closely related but visually very different maple species to better understand the possible photoprotective functions of anthocyanins. To see if anthocyanins protect chloroplasts, especially PSII, from high light, we investigated the pigment composition, photosynthetic reactions, PSII photoinhibition and

accumulation of carbon-centered radicals. Further, we studied the degradation of thylakoid protein complexes with native gel electrophoresis, (i) to see how the components of the photosynthetic electron transport chain are degraded during autumn senescence in the two Norway maple varieties, and (ii) to see if high anthocyanin content affects the degradation process.

2 | MATERIALS AND METHODS

2.1 | Plant material

Leaves from Norway maple (*A. platanoides* L.; green maple), and from its purple-colored variety (Faassen's black; purple maple) were collected on September 20, 2022–October 24, 2022, from trees growing on urban areas of Turku (Finland). Leaves of green maple were collected from trees that turned yellow or only slightly red during the autumn senescence; consequently, non-senescing leaves appeared green and senescing leaves pale green or yellow (see Figure S1). On the other hand, non-senescing leaves of Faassen's black often appeared deep purple or even almost black and senescing leaves red or bright orange (Figure S1). After collection, leaves were brought to the laboratory for analyses. A set of non-senescing and senescing leaves was always collected at the same time from a single tree. All experiments were conducted with leaf material collected from at least three individual trees.

Pumpkin (*Cucurbita maxima* Duchesne) was grown in a greenhouse, as described in Mattila et al. (2023).

2.2 | Chlorophyll *a* fluorescence

$(F_M-F_0)/F_M = F_V/F_M$ values were measured with FluorPen (Photon Systems Instruments) from adaxial leaf surfaces (unless otherwise mentioned) after at least 30 min dark-acclimation. Rapid light curves and quenching analyses were performed with Multi-Color-PAM (Walz) on light-acclimated leaves. Fluorescence was probed with a low-intensity (setting 3) measuring beam (625 nm; 5000 Hz). Leaves were illuminated with white light of photosynthetic photon flux densities (PPFD) of 1, 4, 28, 54, 80, 119, 232, 328, 432, 674, 800, 1125, 1499, 1771, and 2045 µmol m^{-2} s^{-1}, 30 s with each PPFD, after which they were incubated in the dark for 4 min. An 800-ms saturating flash (setting 20) was given at the end of each PPFD and every 1 min under the darkness to calculate the relative electron transfer rate (ETR; PPFD*0.42*$(F_M'-F)/F_M'$), photochemical quenching (qL; $(F_M'-F)/(F_M'-F_0')*(F_0'/F)$; Kramer et al., 2004), regulated non-photochemical quenching (NPQ; $F/F_M'-F/F_M$) and non-regulated non-photochemical quenching (NO; F/F_M) of fluorescence. An estimate for F_0' (Oxborough & Baker, 1997) was used. Minimum saturating irradiance and α (the initial slope of the light curve) were obtained by fitting the data to a model of Platt et al. (1980) in the Pam-Win-3 software (Walz). Red-measuring beam was chosen so that the high anthocyanin content of Faassen's black would not disturb the fluorescence measurements, while white light was used as actinic illumination to stimulate natural conditions.

2.3 | Photoinhibition experiments

Leaf pieces (approximately 2 × 3 cm) were placed, either adaxial or abaxial side up (as indicated) on a wet paper on a temperature-controlled metal block (set to 20°C) and illuminated (PPFD 2000 µmol m^{-2} s^{-1}) for 45 min with a sunlight simulator LED lamp (SLHolland). After the light treatment, leaf pieces were left to recover under low light (PPFD approximately 2 µmol m^{-2} s^{-1}) for 3 h. Photoinhibition was quantified by the F_V/F_M parameter, measured with FluorPen (Photon Systems Instruments) from the illuminated side of the leaf, after 30 min dark-acclimation. In the case of Faassen's black, some of the leaf pieces were dropped from the experiments due to too low F_V/F_M values (prior an illumination).

2.4 | Isolation of thylakoid membranes

Three individual isolations were conducted from three trees (for both green and Faassen's black maple). Leaves were kept under darkness for at least 30 min prior the isolation (for the F_V/F_M measurements), after which main veins were removed, rest of the leaf material was cut to pieces and shortly ground with a blender in cold isolation buffer (50 mM Hepes/KOH (pH 7.5), 330 mM sorbitol, 5 mM $MgCl_2$, 1% (w/v) bovine serum albumin, 5 mM sodium-L-ascorbate, 5% (w/v) polyethylene glycol, 10 mM sodium fluoride (NaF)). Ascorbate was added right before the isolation. The mixture was filtered through Miracloth (Merck Millipore) and centrifuged (5 min, 5000 × *g*, 4°C). Supernatant was removed and the pellet was resuspended in an osmotic shock buffer (50 mM Hepes/KOH (pH 7.5), 5 mM $MgCl_2$, 10 mM NaF) and centrifuged (5 min, 5000 × *g*, 4°C). Supernatant was removed and the pellet washed with storage buffer (50 mM HEPES/KOH (pH 7.5), 100 mM sorbitol, 5 mM $MgCl_2$ and 10 mM NaF), followed by centrifugation (5 min, 5000 × *g*, 4°C). Finally, the pellet was resuspended in the storage buffer and stored at −75°C before use.

Pumpkin thylakoids were isolated without NaF, ascorbate or polyethylene glycol, as described in Mattila et al. (2023).

2.5 | Determination of the protein amount

10 µL of thylakoid suspension was dissolved in 30 µL of a protein isolation buffer (50 mM Tris–HCl (pH 8.0), 2% sodium dodecyl sulfate, 10 mM ethylenediaminetetra-acetic acid), the sample was frozen in liquid nitrogen and then immediately melted (75°C). Freezing/melting was repeated, after which the sample was centrifuged (10 min, 18,000 × *g*). The amount of total proteins was determined with the Lowry method, using the DCTM Protein assay kit (Bio-Rad). A calibration curve was obtained with bovine serum albumin.

2.6 | Quantification of pigments

Pigments were extracted from leaf pieces in dimethylformamide (by incubating the sample for several days in the dark at 4°C) and from thylakoids in 80% acetone (pH 7.5). Chlorophylls and carotenoids were then quantified with a spectrophotometer according to Porra et al. (1989) and Wellburn (1994), respectively. Leaf chlorophyll amount was also estimated by MultispeQ (PhotosynQ) using the optical SPAD method (Hunt & Daughtry, 2014; Mattila & Tyystjärvi, 2023). In this case, the relative chlorophyll values measured with MultispeQ were converted to μg cm^{-2} with an empirical calibration curve (Figure S2).

2.7 | Leaf weight and thickness

Leaf thickness was first determined with MultispeQ (PhotosynQ), which uses a Hall effect sensor. After that, leaf pieces (3 × 0.28 cm^{-2}) cut from the same leaf area were immediately weighed with an analytical scale.

2.8 | Detection of carbon-centered radicals

Thylakoids (50 μg chlorophylls mL^{-1}) were illuminated for 30 min (PPFD 2000 μmol m^{-2} s^{-1} with a cold white LED) at 20°C with constant mixing in the presence of 50 mM α-(4-pyridyl 1-oxide)-*N*-tert-butylnitrone (POBN; Enzo Life Sciences Inc.), as described in Mattila et al. (2023). Accumulation of carbon-centered radicals (POBN-R adduct) was measured before and after the treatment with an EPR spectrometer (Miniscope MS 5000; Magnettech GmbH) and quantified by calculating the height of the first positive peak, as described in Mattila et al. (2023).

2.9 | Polyacrylamide gel electrophoresis

The sample preparation for blue native (BN)-polyacrylamide gel electrophoresis (PAGE), gel casting and electrophoresis were done essentially as described in Järvi et al. (2011) and Rantala et al. (2018). Briefly, the isolated thylakoid samples were diluted in BTH buffer (25 mM Bis/Tris/HCl (pH 7.0), 20% (w/v) glycerol, 0.25 mg mL^{-1} Pefabloc and 10 mM NaF). An equal volume of 4% β-dodecyl-maltocide (DM, Sigma) in BTH buffer was added to the sample to achieve a final concentration of 0.5 mg mL^{-1} of chlorophyll and 2% DM. The samples were solubilized for 2 min on ice and the unsolubilized membrane debris was removed by centrifugation at 18,000 × *g* at 4°. After centrifugation, 1/10 (v/v) of Serva Blue buffer (100 mM BisTris/HCl (pH 7.0), 0.5 M ACA, 30% (w/v) sucrose and 50 mg mL^{-1} Serva Blue G) was added to the sample and 8 μg of chlorophyll was loaded on each well. Two-dimensional sodium dodecyl sulfate (2D-SDS)-PAGE analysis of protein complexes was performed as described in Rantala et al. (2018). The proteins were visualized by silver staining (Blum et al., 1987).

2.10 | Statistical analyses and figure preparation

Data fitting and statistical tests (Student's *t*-tests, heteroscedastic) were performed in Microsoft Excel (Office). Figures were prepared with SigmaPlot (Systat) and CorelDraw (Alludo).

3 | RESULTS

3.1 | Pigment compositions and PSII efficiency in autumn leaves of green and purple Norway maple

Non-senescing (mature) and senescing leaves were collected during autumn from outdoor grown trees of Norway maple (denoted here as "green") and from its purple-colored variety (Faassen's black; denoted as "purple"). The advancement of senescence was estimated by measuring the chlorophyll content of the leaf. In general, non-senescing purple leaves contained more chlorophyll (per leaf area) than non-senescing green maple leaves. Accordingly, non-senescing purple leaves were slightly thicker and heavier than those of green maple (Figure 1A,B). In the case of green maple, senescing leaves were thinner and lighter than non-senescing leaves (Figure 1B). On the other hand, chlorophyll content did not significantly affect the fresh weight of purple leaves (Figure 1B). In green maple, F_V/F_M values, measured after 30 min in the dark, remained high (>0.7) even in senescing leaves with very little chlorophyll left (Figure 1C). Non-senescing purple leaves also showed high F_V/F_M values (approximately 0.8); however, low F_V/F_M values (approximately ranging from 0.1 to 0.6) were measured from a large proportion of senescing purple leaves (Figure 1C).

To get more specific information about the pigment contents of the leaves, pigments were extracted and quantified with a spectrophotometer (Figure S3A). The chlorophyll *a*-to-*b* ratio was lower in purple leaves than in green leaves (Figure 2). During senescence, the ratio slightly decreased in both the green and purple maple (Figure 2). The carotenoids-to-chlorophylls ratio increased during senescence, again in both the green and purple maple; however, the increase was more pronounced in purple leaves (Figure 2).

3.2 | In purple maple, F_V/F_M decreased slowly during high light treatment but senescing leaves possessed poor recovery capacity

To understand the reasons behind the low F_V/F_M values of senescing purple leaves (Figure 1C) and, in general, to test the capacity of green and purple maple leaves to resist PSII photoinhibition, leaf pieces were illuminated with high light. Before and after the treatment, PSII activity was estimated with the fluorescence parameter F_V/F_M. The senescing leaves of purple maple had low F_V/F_M values already before any illumination (Figures 1C and 3) and, therefore, it was necessary to quantify photoinhibition as a percentage of the remaining PSII activity (compared to control; Table 1) to compare the amount of PSII

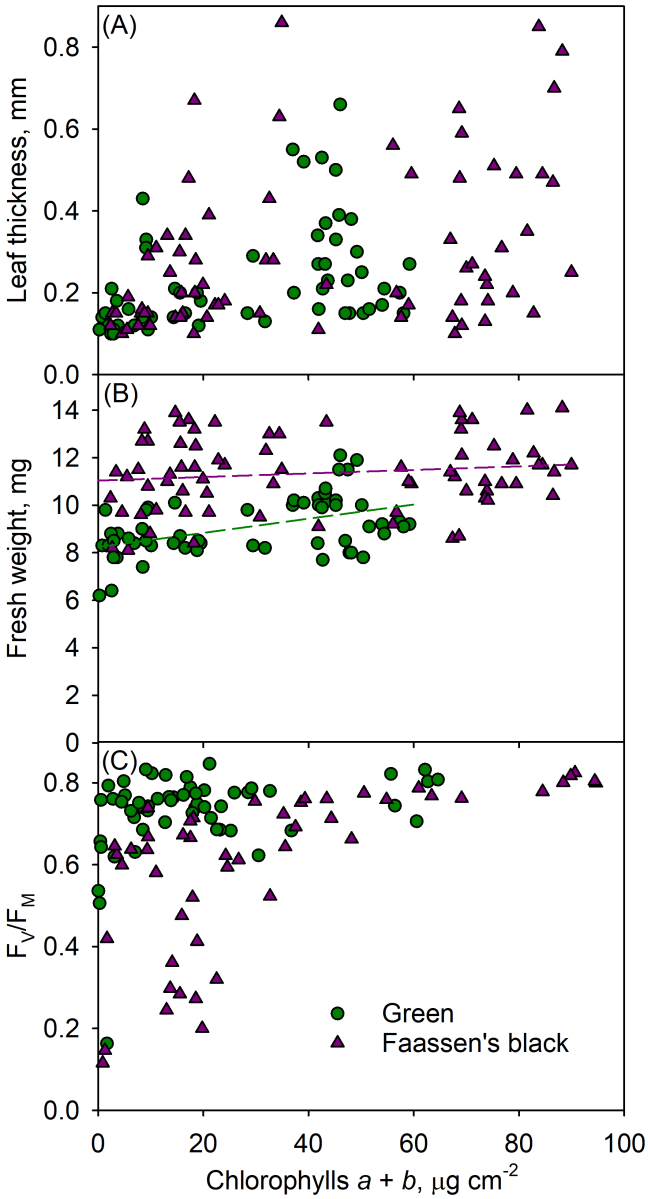

FIGURE 1 Thickness (A), fresh weight (B), and F_V/F_M values (C) measured from non-senescing and senescing leaves of Norway maple (Green; green circles) and from its purple-colored variety (Faassen's black; violet triangles). Dashed lines (B) show the best fits to linear equations. Measurements in (C) have been conducted after 30 min of dark acclimation. Chlorophyll contents were estimated with an optical method and converted to μg cm^{-2} with an empirical calibration curve (see Figure S2). Each data point shows an individual measurement ($n = 57$ in the case of green maple and $n = 72$ in the case of purple maple) collected from at least five individual trees (A, B) and ($n = 57$ in the case of green maple and $n = 50$ in the case of purple maple) collected from three individual trees (C).

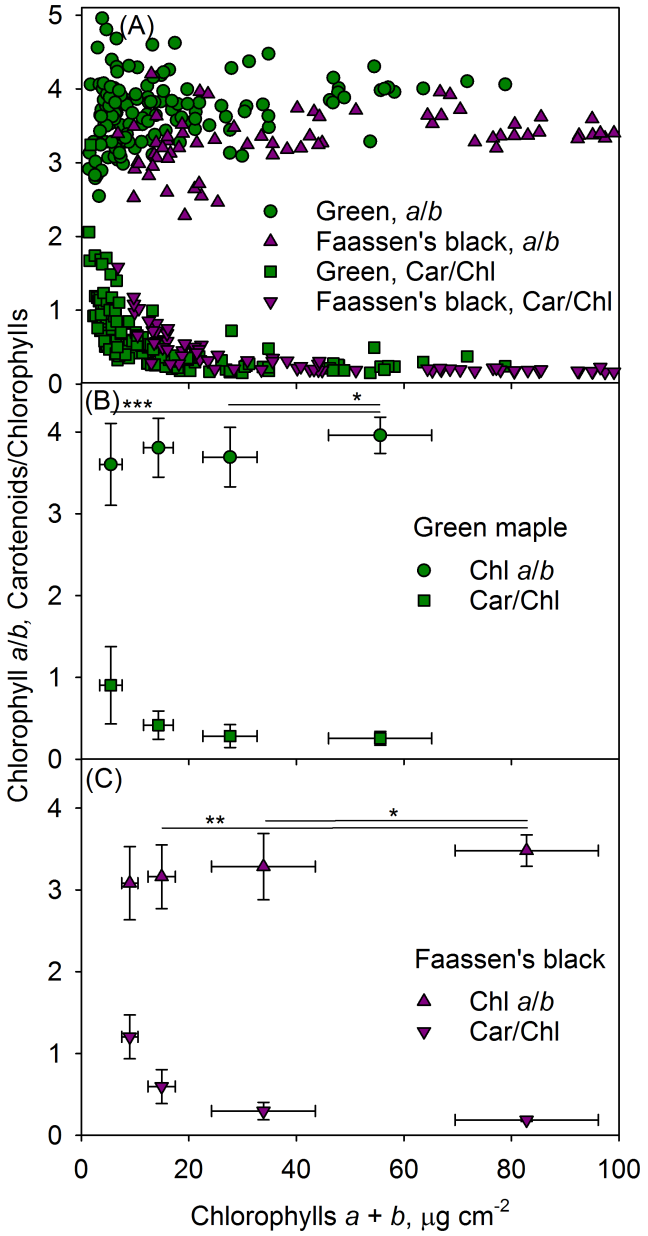

FIGURE 2 Ratios of chlorophylls (Chl) *a*-to-*b* (circles and upwards triangles) and of carotenoids (Car)-to-chlorophylls (squares and downward triangles) in non-senescing and senescing leaves of Norway maple (Green; green symbols) and in its purple-colored variety (Faassen's black; violet symbols). Data show individual measurements ($n = 138$ in the case of green maple and $n = 71$ in the case of purple maple) collected from at least 10 individual trees (A) or average values of the data, divided for easier visualization into groups corresponding to non-senescing leaves with the highest chlorophyll content and to three stages of senescence (B, C). Error bars show SD. Statistically significant differences (Student's *t*-tests, heteroscedastic) between the indicated groups are highlighted with asterisks (calculated only for Chl *a*/*b* values). Statistical significances (probability of the null hypothesis) of $p < 0.001$ are indicated with ***; $p < 0.01$ with ** and $p < 0.05$ with *.

inactivation that was due to the light treatment in green and purple maple. The high-light-induced decrease in the F_V/F_M value was smaller in purple leaves than in green maple, both in the case of non-senescing and senescing leaves (Figure 3; Table 1). Non-senescing leaves of purple maple also recovered better, during a low-light incubation after the high-light treatment, compared to green non-senescing leaves. However, senescing purple leaves recovered very little during the low-light incubation (Figure 3; Table 1).

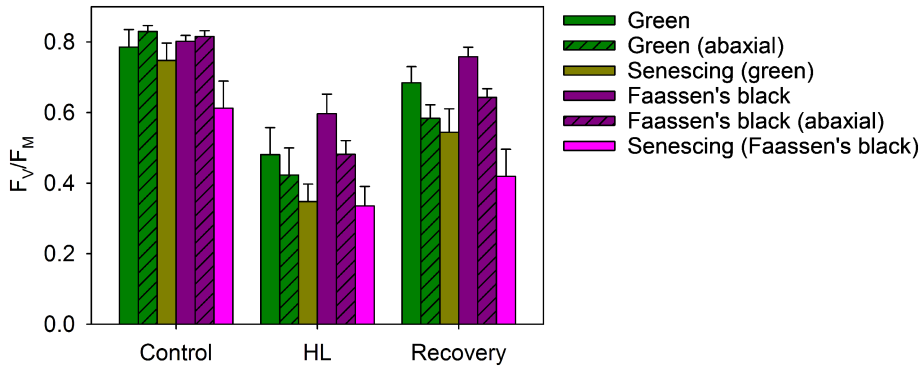

FIGURE 3 Photoinhibition and recovery in non-senescing (green) and senescing (dark yellow) leaves of Norway maple (Green) and in non-senescing (violet) and senescing (pink) leaves of its purple-colored variety (Faassen's black). Leaf pieces were illuminated with high light (HL), either on the adaxial (open bars) or on the abaxial leaf surface (when indicated; hatched bars), after which they were left to recover for a few hours under low light. F_V/F_M values were measured after 30 min in the dark. Control shows the values prior to the illumination. Data show averages ($n = 6$ in the case of non-senescing leaves and $n = 9$ in the case of senescing leaves, collected from three individual trees) and error bars show SD.

TABLE 1 Chlorophyll contents, F_V/F_M values after high light and recovery (as percentages of the control), as well as the amounts of recovery (as percentages of photoinhibition) of the leaf pieces used in the photoinhibition experiment (Figure 3). Averages ± SD are shown. Different letters indicate a statistically significant difference; the tests were conducted between non-senescing leaves (green vs. Faassen's black; both adaxial and abaxial illumination), between non-senescing and the corresponding senescing leaves, between senescing leaves (green vs. Faassen's black) and between adaxial and abaxial illuminations (green vs. green and Faassen's black vs. Faassen's black). Chlorophyll contents were estimated with an optical method and converted to μg cm^{-2} with an empirical calibration curve (see Figure S2).

Leaves	Chlorophyll, μg cm^{-2}	F_V/F_M after high light, % of control	F_V/F_M after recovery, % of control	Recovery, % of inhibition
Green	60.3 ± 3.6	61.5 ± 11[a]	87.2 ± 4.7[a]	65.9 ± 10.5[a]
Senescing (green)	19.0 ± 8.1	46.8 ± 7.9[b]	72.9 ± 8.2[b]	49.3 ± 12.9[b]
Faassen's black	92.7 ± 8.3	74.4 ± 6.6[b]	94.6 ± 2.7[c]	78.9 ± 8.1[b]
Senescing (Faassen's)	18.4 ± 9.0	54.9 ± 6.5[c]	68.3 ± 6.5[b]	29.4 ± 12.6[c]
Green, abaxial	56.3 ± 7.2	50.8 ± 8.3[a,d]	70.3 ± 3.7[d]	38.7 ± 9.7[a]
Faassen's black, abaxial	80.6 ± 6.1	59.1 ± 5.9[d]	78.9 ± 3.7[e]	48.2 ± 6.0[a]

Senescing leaves of green and purple maple contained, on average, similar amounts of chlorophyll (Table 1). Non-senescing purple leaves, on the other hand, contained notably more chlorophyll than non-senescing green leaves (Table 1), which could contribute to the observed photoinhibition tolerance of these leaves as, in a leaf with high chlorophyll content, the upper cell layers can efficiently shield chloroplasts in the lower cell layers. Therefore, to estimate the effect of the higher chlorophyll content of purple leaves on photoinhibition, non-senescing leaves were also illuminated on the abaxial, non-anthocyanic leaf surface (see Figure S1C), in which case anthocyanins should exert a minimal effect on photoinhibition. In line with the measurements conducted on the adaxial surfaces with non-senescing leaves, purple maple was more resistant against photoinhibition and showed better recovery capacity than green maple (Figure 3). The differences, however, were smaller than in the case of adaxial illumination and not statistically significant, except in the case of the F_V/F_M values after the recovery (Table 1).

3.3 | Photochemical and non-photochemical quenching and initial slope of the light curve (α) were low in senescing leaves

To estimate the photosynthetic capacity of non-senescing and senescing leaves of green and purple maple, and to determine if induction of non-photochemical quenching differed in the leaves with different amounts of chlorophyll and anthocyanins, rapid light response fluorescence curves were measured from light-acclimated leaves (Figure 4; Figure S5). As light absorption by PSII in the different leaves was not known, only relative ETR could be calculated (Figure 4B). Based on the ETR curves, minimum saturating irradiance and α (the initial slope of the light curve) were calculated. Minimum saturating irradiances were slightly higher in purple than in green maple (but the differences were not statistically significant; Figure 4C). The values of the α parameter were lower in senescing leaves than in non-senescing leaves, though the differences were statistically significant only in the case of purple leaves (Figure 4D). Photochemical quenching (qL) was

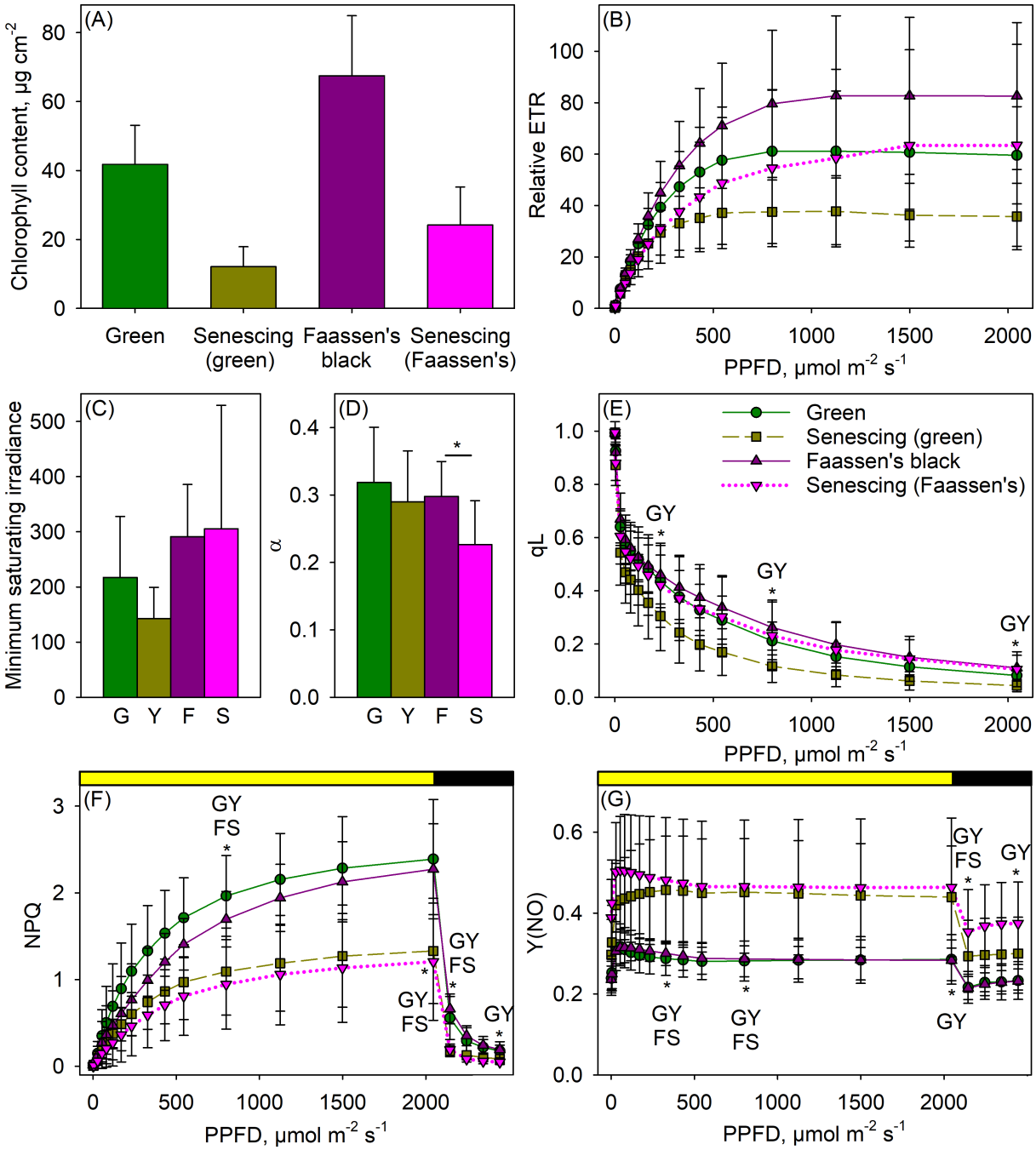

FIGURE 4 Rapid light response fluorescence curves measured from light-acclimated non-senescing (green continuous lines) and senescing (dark yellow dashed lines) leaves of Norway maple (Green) and from light-acclimated non-senescing (violet continuous lines) and senescing (pink dotted lines) leaves of its purple-colored variety (Faassen's black). (A) Chlorophyll contents were estimated with an optical method and converted to µg cm^{-2} with an empirical calibration curve (see Figure S2). (B) Relative electron transfer rates (ETR) at the indicated light intensities. (C) Minimum saturating irradiances and (D) α (initial slopes of the light curve), calculated based on (B). (E) Photochemical (qL), (F) non-photochemical (NPQ), and (G) the yield of non-regulated non-photochemical (NO) quenching of chlorophyll fluorescence at the indicated light intensities (yellow horizontal bar) or under subsequent darkness (black bar). Statistically significant differences (Student's *t*-tests, heteroscedastic) at the PPFDs 170, 800, and 2045 µmol m^{-2} s^{-1} and after 60 and 240 s of dark-acclimation are highlighted with asterisks. Statistical significances (probability of the null hypothesis) of $p < 0.001$ are indicated with ***; $p < 0.01$ with **; $p < 0.05$ with *. The tests were performed between non-senescing leaves, between non-senescing and corresponding senescing leaves and between senescing leaves. F, Faassen's black; G, Green; S, Senescing (Faassen's black); Y, Senescing (green). Data show averages ($n = 9$, collected from nine individual trees) and error bars show SD. For examples of the original fluorescence curves, see Figure S4.

lower in senescing leaves of both green and purple maple, as compared to the non-senescing leaves (Figure 4E). Furthermore, qL was lower in green maple than in purple maple, particularly in the senescing leaves, almost at all tested light intensities (Figure 4E). However, the lower average chlorophyll content of green leaves, compared to purple leaves (Figure 4A), makes the direct comparison more difficult, especially in the case of senescing leaves. NPQ was higher and NO lower in non-senescing than in senescing leaves in both green and purple maples (Figure 4F,G). In general, NPQ was slightly lower in purple than in green maple leaves (but the difference was not statistically significant), which together with the high qL, contributed to the high relative ETR values in purple leaves.

3.4 | Pigment analysis from isolated thylakoid membranes

Next, to study the degradation of the photosynthetic machinery during senescence, thylakoid membranes were isolated from non-senescing and senescing leaves. In the case of green maple, two classes of senescing leaves, "early" (approximately 35% of chlorophylls left, compared to non-senescing leaves) and "late" (approximately 15% of chlorophyll left), were used (Table 2). Senescing purple leaves were selected so that their chlorophyll content approximately corresponded to the chlorophyll content of the early senescing green leaves (Table 2). As observed before (Figures 1 and 2), senescing purple maple showed low F_V/F_M values, a low chlorophyll *a*-to-*b* ratio, and a high carotenoids-to-chlorophylls ratio, compared to senescing green maple (Table 2; Figure S3B). The protein-to-chlorophyll ratio increased in senescing leaves, compared to non-senescing leaves, though the difference was statistically significant only in the case of purple maple (Table 2).

3.5 | Analysis of the senescence-related decline of photosynthetic protein complexes

The degradation of the photosynthetic protein complexes upon autumn senescence was assessed from the thylakoids isolated from senescing leaves of green and purple maple (Figure 5; Table 2). The photosynthetic protein complexes were excised from the thylakoid membranes using the mild, non-ionic detergent β-DM that solubilizes membrane protein complexes in their native form (i.e., still associated with the pigments). Protein complexes were then separated on blue native (BN)-PAGE and the gel was stained with Coomassie dye for better visibility of the complexes (Figure 5A,C). For protein complex identification, the protein subunits of the isolated protein complexes were separated using denaturing two-dimensional (2D)-SDS-PAGE (Figure 5B,D).

In the thylakoids isolated from non-senescing green maple leaves, four large PSII-LHCII supercomplexes, PSII dimer/PSI-LHCI, ATPase, PSII monomer, Cyt b_6f, M-LHCII, and LHCII trimer were resolved (Figure 5A). In the thylakoids isolated from early senescing leaves, the amount of the four PSII-LHCII supercomplexes decreased dramatically (Figure 5A). The amount of the PSII core dimer decreased slightly, whereas the PSI, Cyt b_6f, and ATPase complexes remained intact during early senescence (Figure 5A,B). The amount of LHCII decreased only marginally (Figure 5A,B). In the thylakoids isolated from late senescing leaves of green maple, almost all PSII complexes were degraded (Figure 5A,B) and also the amount of PSI, Cyt b_6f, ATPase, and LHCII significantly decreased (Figure 5A,B).

The pattern of the photosynthetic membrane protein complexes in the thylakoids isolated from leaves of non-senescing Faassen's black maple was similar to the non-senescing green maple (Figure 5). In the senescing purple maple, almost all PSII supercomplexes were disassembled (Figure 5C) and almost all PSII units were degraded (Figure 5C,D). The amount of PSI, ATPase, and Cyt b_6f was also significantly decreased, while high amounts of LHCII remained intact (Figure 5C,D). Since the chlorophyll content of the senescing purple maple corresponded to the chlorophyll content of the early senescing green maple, the degradation of the photosynthetic protein complexes seemed to proceed notably faster in purple maple than in green maple during the autumn senescence.

3.6 | Very little carbon-centered radicals were detected from maple thylakoids

Finally, the accumulation of carbon-centered radicals in the thylakoids during a high light illumination was measured to get more insights into the production of reactive oxygen species during autumn

TABLE 2 Chlorophyll (Chl) contents and F_V/F_M values (measured after 1 h dark-acclimation) measured from non-senescing and senescing leaves of Norway maple (Green) and from its purple-colored variety (Faassen's black) used for isolation of thylakoid membranes, and ratios of chlorophylls *a* to *b*, of chlorophylls to carotenoids (Car) and of chlorophylls to proteins, measured from the thylakoids. Different letters indicate a statistically significant difference; the tests were performed between non-senescing leaves (green vs. Faassen's black), between non-senescing and the corresponding senescing leaves and between senescing (early) and senescing (Faassen's black). Averages ± SD are shown.

Leaves	Chl, μg cm^{-2}	F_V/F_M	Chl *a*/*b*	Car/Chl	Protein/Chl
Green	48.4 ± 9.8	0.79 ± 0.01^{a}	2.95 ± 0.14^{a}	0.18 ± 0.01^{a}	9.8 ± 1.2^{a}
Senescing (early)	17.0 ± 2.9	$0.76 \pm 0.04^{a-c}$	3.07 ± 0.09^{a}	0.25 ± 0.03^{b}	$14.7 \pm 2.9^{a,b}$
Senescing (late)	7.5 ± 2.6	0.75 ± 0.003^{b}	3.07 ± 0.13^{a}	$0.37 \pm 0.08^{b,c}$	22.3 ± 10.3^{a}
Faassen's black	71.9 ± 11.1	$0.77 \pm 0.03^{a,c}$	$2.62 \pm 0.05^{b,c}$	$0.18 \pm 0.01^{a,d}$	7.6 ± 0.9^{a}
Senescing (Faassen's)	20.6 ± 6.2	0.58 ± 0.13^{c}	2.62 ± 0.08^{c}	0.34 ± 0.01^{e}	17.1 ± 2.1^{b}

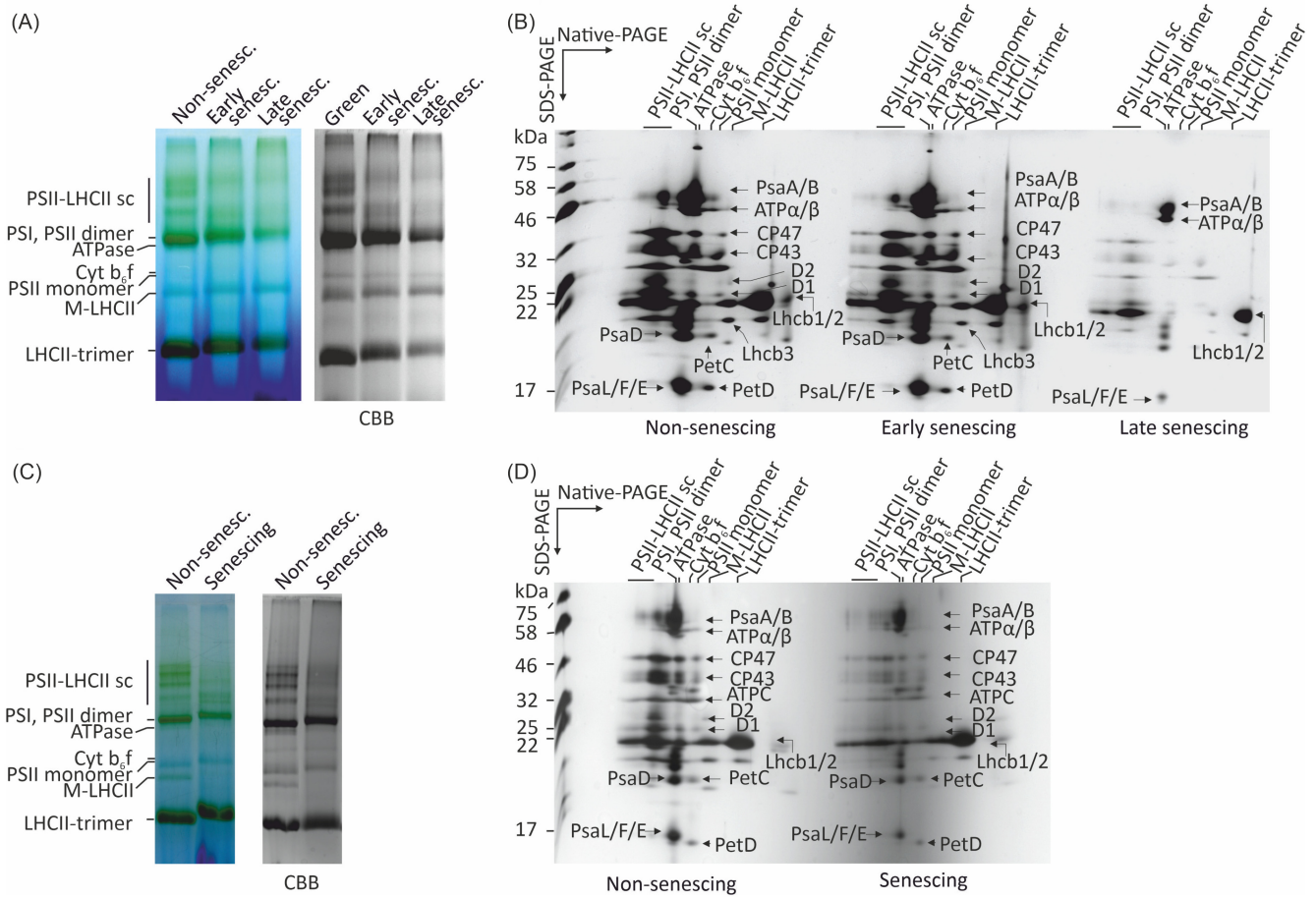

FIGURE 5 Separation of the thylakoid membrane protein complexes, with BN and 2D-SDS-PAGE, isolated from non-senescing and senescing (early/late) leaves of green Norway maple (A, B) and from its purple-colored variety (Faassen's black; C, D), as indicated. (A, C) The thylakoids were solubilized with β-DM and 8 μg of chlorophyll was loaded on each well. After electrophoresis, the gels were stained with a Coomassie (CBB) stain for better visibility. (B, D) Gel lanes from native PAGE were incubated in denaturing Laemmli buffer and individual subunits were separated according to their size with SDS-PAGE. The proteins were visualized with silver stain and the protein subunits annotated based on Aro et al. (2005). Sc, supercomplex. For a general characterization of the leaves and thylakoids, see Table 2. For two additional biological repetitions (from different trees), see Figure S5.

senescence. Carbon-centered radicals are produced by ROS mediated lipid and/or protein oxidation and have been suggested to also originate from the formation of oxidized PSII reaction center chlorophyll ($P680^+$), which both have the potential to cause photoinhibition. Compared to thylakoids isolated from greenhouse-grown pumpkins, very little radical accumulation was detected in maple thylakoids, regardless if they were isolated from green or purple leaves or from non-senescing or senescing leaves (Figure 6). Slightly more radicals were detected in thylakoids isolated from non-senescing purple leaves than in thylakoids isolated from non-senescing green maple. No statistically significant differences were found between senescing and non-senescing thylakoids (Figure 6).

4 | DISCUSSION

In the present research, we studied pigment composition, biophysical characteristics, and degradation of the photosynthetic protein complexes during natural autumn senescence in a deciduous species, Norway maple (*A. platanoides* L.). In addition to the common, green-colored variety, another variety of Norway maple that contains purple leaves throughout the season (Faassen's black), was used to dissect the possible roles of anthocyanins in photoprotection during senescence.

4.1 | PSII activity drops in senescing Faassen's black leaves due to poor PSII recovery

Faster PSII photoinhibition was observed in both senescing and non-senescing leaves of green maple than in purple maple (Figure 3; Table 1). The difference in photoinhibition tolerance between non-senescing leaves of purple and green maple greatly diminished when illumination was done on the non-anthocyanic abaxial leaf surface (see Figure S1) and we, therefore, suggest that the high anthocyanin content of purple leaves contributed to their photoinhibition

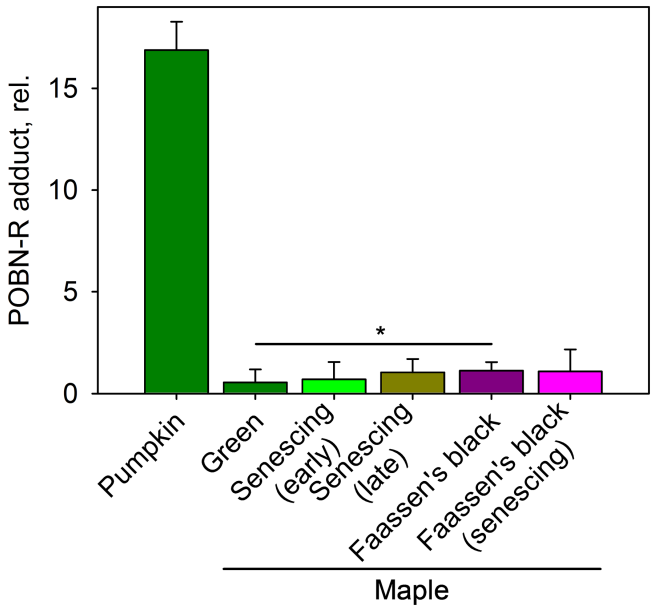

FIGURE 6 Accumulation of carbon-centered radicals (R) during a high light illumination in thylakoid membranes, isolated from greenhouse-grown pumpkin and from non-senescing and senescing leaves of Norway maple (Green) and of its purple-colored variety (Faassen's black), as indicated. Radicals were detected with an EPR probe (POBN). The signal obtained prior to the illumination has been subtracted from the results. A statistically significant difference (Student's *t*-tests, heteroscedastic) between the indicated maple groups is highlighted with an asterisk. Statistical significances (probability of the null hypothesis) of $p < 0.001$ are indicated with ***; $p < 0.01$ with **; $p < 0.05$ with *. Data show averages ($n = 3$, collected from three individual trees, except in the case of pumpkin where leaves from three individual plants were pooled) and error bars SD. For a general characterization of the leaves and thylakoids, see Table 2.

tolerance, in the case of both non-senescing and senescing leaves. However, it cannot be excluded that other differences, besides the anthocyanin content, such as the high carotenoid content of senescing purple maple (Figure 2), contributed to the observed photoinhibition results. While the non-senescing leaves of purple maple showed faster recovery from photoinhibition than non-senescing green maple, almost no recovery was observed in the senescing purple leaves (Figure 3). Therefore, it is postulated that anthocyanins, although they diminished PSII damage during the high-light treatment via shielding, did not protect the PSII repair process in senescing leaves. It is known that the PSII repair cycle is sensitive to reactive oxygen species (Bethmann et al., 2019; Nishiyama et al., 2001; Yutthanasirikul et al., 2016). Thus, the previous observations of no differences between the antioxidant capacities of anthocyanic and non-anthocyanic Norway maple and sugar maple leaves (Duan et al., 2014; van den Berg & Perkins, 2007) are in agreement with our suggestion that anthocyanins did not protect PSII repair.

In the senescing leaves of green maple, PSII activity remained high (F_V/F_M 0.7–0.8; measured before any high light treatments) until the point where almost no chlorophyll was left (Figure 1C), in line with previous reports (e.g., Keskitalo et al., 2005; Mattila et al., 2021; Moy et al., 2015). On the contrary, despite its slower photoinhibition, a dramatic decrease in PSII activity (measured before any high light treatments) co-occurred with the chlorophyll degradation in the purple maple (Figure 1C). We suggest that, due to its low recovery capacity (Figure 3), damaged PSII units accumulated in the senescing leaves of purple maple. If the poor PSII repair capacity is a common feature of red leaves, this result may explain the apparent discrepancy between previous observations of low F_V/F_M values (e.g., Nikiforou et al., 2011) and high tolerance against photoinhibition of PSII (e.g., Hoch et al., 2003) in leaves with high anthocyanin content.

In agreement with our hypothesis on the involvement of anthocyanins in photoprotection, another study showed that in-canopy leaves of senescing fullmoon maple (*Acer japonicum*) containing low anthocyanin levels were more vulnerable to PSII damage under high light compared to anthocyanin-rich outer-canopy leaves (Kitao et al., 2022). However, other differences between the studied leaf types (high light vs. low light acclimated leaves) could also have contributed to the observed vulnerability to photoinhibition. On the other hand, no significant photoprotection by red pigments was found when red and yellow leaf sections of senescing Norway maple (the common variety, here denoted as "green") were compared (Mattila & Tyystjärvi, 2023). The contrasting results on the role of anthocyanins in PSII photoprotection may be explained by the differences in the extent and timing of anthocyanin synthesis in different plant species. Norway maple trees usually accumulate less anthocyanins and at a later phase of senescence (Mattila & Tyystjärvi, 2023) than fullmoon maple (Kitao et al., 2022) or the purple Faassen's black that accumulates high amounts of anthocyanins already before senescence (Figure S1).

4.2 | PSII degradation precedes the decline of other photosynthetic complexes in both green and purple maple during senescence, but the degradation is faster in purple maple

Our analysis of the native thylakoid protein complexes during autumn senescence demonstrates that PSII-LHCII supercomplexes, containing PSII core dimer and two to four copies of trimeric LHCII complexes, are the first to disassemble during autumn senescence in both green and purple maple (Figure 5). The disassembly of PSII-LHCII supercomplexes is considered to be prerequisite for the degradation of the PSII core subunits (Huang et al., 2013). Here, such disconnection of LHCII from the PSII core in early senescing green maple was accompanied by only a small decrease in the amount of PSII core proteins (Figure 5B), which started to degrade dramatically only in the late senescing leaves (Figure 5A,B). In the purple maple, on the other hand, the disassembly of the PSII-LHCII supercomplex was accompanied by degradation of the PSII core subunits (Figure 5C,D), and the overall degradation of the photosynthetic complexes was much faster than in green maple. In both green and purple maple, high amounts of LHCII remained undegraded during the senescence (Figure 5). Early degradation of the LHCII antenna and PSII has been reported in other non-

deciduous species (Tang et al., 2005; Wang et al., 2014) and can indeed occur independently of each other (Chen et al., 2021).

In both the green and purple maple, we observed faster degradation of PSII than PSI (Figure 5). This contrasts the observations of Moy et al. (2015), who observed faster degradation of PSI compared to that of PSII in sugar maple and in swamp white oak during autumn senescence. However, also Moy et al. (2015) observed that when the PSII inner antenna protein CP43 was completely degraded at a late phase of senescence in oak, the PSI protein PsaB was still detected. Thus, it may not be enough to measure a single time point during senescence. According to Moy et al. (2015), Lhcb1, Lhcb2, and Lhcb5 were retained, while Lhcb3, Lhcb4, and Lhcb6 were degraded faster. We also observed the slow degradation of Lhcb1 and Lhcb2 (Figure 5).

In many tree species, chlorophyll *a*-to-*b* ratio decreases during autumn senescence (Lee et al., 2003; Moy et al., 2015; Wolf, 1956), suggesting that a common strategy during autumn senescence is to first degrade photosystem core complexes and only later the chlorophyll *b* enriched LHCII. However, in some tree species, for example in striped maple (*Acer pensylvanicum*) and in sycamore maple, the chlorophyll *a*-to-*b* ratio increases during senescence (Fulgosi et al., 2012; Lee et al., 2003; Mattila et al., 2021). Our pigment analyses demonstrate that the chlorophyll *a*/*b* ratio only slightly decreased during senescence, both in green and purple maple (Figure 2), which is surprising as, particularly during the late senescence, very little of the core complexes were observed, while considerable amount of LHCII was still detected (Figure 5). Thus, simple chlorophyll *a*/*b* ratio analyses are not sufficient to make assumptions about the order in which the photosynthetic complexes are degraded.

We observed that ATPase was retained in the senescing maple leaves (Figure 5), highlighting the need to produce energy during senescence, presumably to power nutrient resorption (Keskitalo et al., 2005). Also, Cyt b_6f stayed intact until late senescence in green maple and was abundant in senescing purple maple. Accordingly, in senescing beech (*Fagus sylvatica*), P700 signal (from PSI) decreases faster than that of Cyt b_6f (Zhu & Wild, 1995), suggesting slow degradation of Cyt b_6f. On the contrary, a limitation was previously observed in the electron transfer to PSI in senescing silver birch leaves, which was speculated to originate from Cyt b_6f or from plastocyanin (Mattila et al., 2021). Plastocyanin amount indeed decreases early during age-related senescence (Shimakawa et al., 2020). However, even very low contents of plastocyanin do not limit photosynthesis in *Arabidopsis thaliana* mutants (Pesaresi et al., 2009). More studies are thus needed to determine if the late degradation of Cyt b_6f is a common feature in autumn senescence.

The differences in the recovery after PSII photoinhibition between the senescing purple and green maple (Figure 3), as discussed above, may stem from the earlier degradation of the photosynthetic electron transfer chain in the purple maple (Figure 5). Indeed, the degradation of the entire photosynthetic machinery seems to be faster and more extensive in purple maple compared to the green maple (Figure 5). Is the "chaotic" degradation of purple maple a symptom or a different senescence strategy? It has been speculated that early degradation of LHCII and PSII may lead to singlet oxygen production during age-related senescence (Krieger-Liszkay et al., 2015; Krupinska et al., 2012). Possibly, the high amounts of anthocyanins and carotenoids could protect leaves from excess light, diminishing singlet oxygen production to a degree that purple maple can afford fast degradation of photosynthetic protein complexes?

4.3 | Why do not purple leaves lose weight during senescence?

Leaf fresh weight decreased with decreasing chlorophyll content in green maple, as commonly occurs during senescence (see the literature collected by van Heerwaarden et al., 2003), but not in purple maple (Figure 1). It has been suggested that anthocyanins work as osmo-regulators (Chalker-Scott, 2002), which could explain the observed difference, as the senescence-associated mass loss may at least partly be due to water loss (Wang et al., 2020). Anthocyanin accumulation is indeed a common response to drought stress and correlates with drought tolerance (for a review, see Naing & Kim, 2021). However, in plants that accumulate anthocyanins during winter, the contribution of anthocyanins to osmotic adjustment is minor compared to other compounds, mainly sugars (Hughes et al., 2013). In senescing leaves of bilberry (*Vaccinium myrtillus*), anthocyanins increased during drought stress, but the increase did not correlate with the severity of the stress and, thus, the authors did not support the osmoregulatory hypothesis (Taulavuori et al., 2010).

4.4 | Thylakoids may not be a significant source of reactive oxygen species during senescence

In this study, we observed only a modest accumulation of carbon-centered radicals in maple thylakoids during illumination, compared to thylakoids isolated from greenhouse-grown pumpkin (Figure 6). Reactive oxygen species have the capacity to oxidize proteins and lipids, which can result in the production of carbon-centered radicals (for a review, see Pospíšil & Yamamoto, 2017). It has been suggested that carbon-centered radicals generated during illumination may also originate from the formation of oxidized PSII reaction center chlorophyll ($P680^+$) or Tyr• (Yadav & Pospíšil, 2012). Plants growing under more harsh outdoors-conditions may possess an ability to quench $P680^+$, maybe via cyclic electron transfer routes around PSII, including cytochrome b_{559} and the β-carotene Car_{D2} (for a review, see Shinopoulos & Brudvig, 2012). Both reactive oxygen species and $P680^+$ have been suggested to cause PSII photoinhibition (Callahan & Cheniae, 1985; Kale et al., 2017; Mattila et al., 2023).

Accumulation of carbon-centered radicals in illuminated thylakoids increased in senescing green maple only a little, compared to thylakoids isolated from non-senescing leaves, and not statistically significantly (Figure 6). Non-senescing purple maple accumulated

slightly more radicals than green maple, but despite the low F_V/F_M and α values and more extensive degradation of protein complexes (Figures 1, 4, and 5), senescing purple maple did not accumulate more carbon-centered radicals than non-senescing purple maple, or senescing green maple. In other studies, more hydrogen peroxide and superoxide have been detected from senescing leaves of several deciduous trees (Cheeseman, 2009; Kraj & Zarek, 2021; Lo Piccolo et al., 2018). Previously, we measured high singlet oxygen production during illumination of senescing silver birch leaves (Mattila et al., 2021). In addition, Lepeduš et al. (2008) observed that oxidation of lipids and especially of proteins increased during autumn senescence in sycamore maple. The above-described measurements (Cheeseman, 2009; Kraj & Zarek, 2021; Lepeduš et al., 2008; Lo Piccolo et al., 2018; Mattila et al., 2021) are conducted on a leaf level and, thus, it may be possible that thylakoid membranes are not the source for the increased reactive oxygen production during senescence. Indeed, production of reactive oxygen species, specifically of singlet oxygen, has been suggested to increase during senescence due to increased enzymatic production (Rangel et al., 2002; Springer et al., 2015), that is, not due to a senescence-associated disruption of light reactions. Also, Shimakawa et al. (2022) proposed that lipid peroxidation observed during early senescence mainly derives from enzymatic oxidation reactions, while at the last stages of senescence, unregulated production of reactive oxygen species increases.

5 | CONCLUDING REMARKS

In the present study, we demonstrate that (i) anthocyanins can indeed protect PSII from light-induced damage in both non-senescing and senescing leaves, provided that they are accumulated in sufficient amounts. Additionally, we show that (ii) the high anthocyanin content does not protect the PSII repair process after photoinhibition during autumn senescence. Instead, (iii) the photosynthetic performance decreases, and (iv) the photosynthetic protein complexes degrade much faster in the anthocyanin-rich purple maple compared to the green maple variety. Thus, the increased protection against photoinhibition in purple maple does not necessarily lead to improved plant fitness.

It is important to note that the purple maple used in this study, Faassen's black, is a garden variety and may not be competitive in a natural environment. Therefore, further research should be conducted using "natural" species to determine if the observations made here can be generalized to other species with high anthocyanin content. Despite this limitation, it is an intriguing observation that purple maple leaves exhibited similar stress symptoms than red leaves of the "green" maple (Mattila & Tyystjärvi, 2023).

There is also another difference between the used maple varieties; non-senescing purple maple leaves are thicker and contain more chlorophyll than those of green maple. Thus, the phase of senescence may not have been the same in the compared senescing leaves, even though they had similar chlorophyll contents, but the senescing leaves of purple maple may have been at a more advanced state of senescence than those of green maple. Therefore, further protein-level studies with deciduous plants are needed to determine if the "chaotic" degradation of the photosynthetic machinery observed in purple maple is an isolated characteristic of a garden plant or a general feature of species with high anthocyanin and/or chlorophyll content.

AUTHOR CONTRIBUTIONS

Marjaana Rantala and Heta Mattila designed and performed the research; all authors analyzed the data; Marjaana Rantala and Heta Mattila wrote the paper with contributions from Paula Mulo and Esa Tyystjärvi.

ACKNOWLEDGMENTS

The Ella and Georg Ehrnrooth Foundation and the Oskari Huttunen Foundation (for Heta Mattila) and the Academy of Finland (grant number 321616 for Marjaana Rantala and Paula Mulo; grant number 333421 for Esa Tyystjärvi) are thanked for financial support. The Finnish Infrastructure for Photosynthesis Research PHOTOSYN is acknowledged for the excellent research facilities.

CONFLICT OF INTEREST STATEMENT

Authors declare no competing interests.

DATA AVAILABILITY STATEMENT

Data will be available upon request from the authors.

ORCID

Marjaana Rantala https://orcid.org/0000-0002-2233-3805
Paula Mulo https://orcid.org/0000-0002-8728-3204
Esa Tyystjärvi https://orcid.org/0000-0001-6808-7470
Heta Mattila https://orcid.org/0000-0002-5071-9721

REFERENCES

Adams, W.W., III, Stewart, J.J. & Demmig-Adams, B. (2018) Photosynthetic modulation in response to plant activity and environment. In: Terashima, I. (Ed.) *The leaf: a platform for performing photosynthesis, advances in photosynthesis and respiration*, Vol. 44. Switzerland: Springer, pp. 493–562.

Agati, G., Guidi, L., Landi, M. & Tattini, M. (2021) Anthocyanins in photoprotection: knowing the actors in play to solve this complex ecophysiological issue. *New Phytologist*, 232, 2228–2235.

Aro, E.M., Suorsa, M., Rokka, A., Allahverdiyeva, Y., Paakkarinen, V., Saleem, A. et al. (2005) Dynamics of photosystem II: a proteomic approach to thylakoid protein complexes. *Journal of Experimental Botany*, 56(411), 347–356.

Bethmann, S., Melzer, M., Schwarz, N. & Jahns, P. (2019) The zeaxanthin epoxidase is degraded along with the D1 protein during photoinhibition of photosystem II. *Plant Direct*, 3, 1–13.

Blum, H., Beier, H. & Gross, H.J. (1987) Improved silver staining of plant proteins, RNA and DNA in polyacrylamide gels. *Electrophoresis*, 8, 93–99.

Callahan, F.E. & Cheniae, G.M. (1985) Studies on the photoinactivation of the water-oxidizing enzyme. I. Processes limiting photoactivation in hydroxylamine-extracted leaf segments. *Plant Physiology*, 79, 777–786.

Chalker-Scott, L. (2002) Do anthocyanins function as osmoregulators in leaf tissues? *Advances in Botanical Research*, 37, 103–106.

Cheeseman, J.M. (2009) Seasonal patterns of leaf H_2O_2 content: reflections of leaf phenology, or environmental stress? *Functional Plant Biology*, 36, 721–731.

Chen, Y., Yamori, W., Tanaka, A., Tanaka, R. & Ito, H. (2021) Degradation of the photosystem II core complex is independent of chlorophyll degradation mediated by stay-green Mg^{2+} dechelatase in Arabidopsis. *Plant Science*, 307, 110902.

Davies, K.M., Landi, M., van Klink, J.W., Schwinn, K.E., Brummell, D.A., Albert, N.W. et al. (2022) Evolution and function of red pigmentation in land plants. *Annals of Botany*, 130(5), 613–636.

Domínguez, F. & Cejud, F.J. (2021) Chloroplast dismantling in leaf senescence. *Journal of Experimental Botany*, 72(16), 5905–5918.

Duan, B., Paquette, A., Juneau, P., Brisson, J., Fontaine, B. & Berninger, F.A. (2014) Nitrogen resorption in *Acer platanoides* and *Acer saccharum*: influence of light exposure and leaf pigmentation. *Acta Physiologiae Plantarum*, 36, 3039–3050.

Field, T.S., Lee, D.W. & Holbrook, M. (2001) Why leaves turn red in autumn. The role of anthocyanins in senescing leaves of RedOsier dogwood. *Plant Physiology*, 127, 566–574.

Fulgosi, H., Ježić, M., Lepeduš, H., Peharec Štefanić, P., Ćurković-Perica, M. & Cesar, V. (2012) Degradation of chloroplast DNA during natural senescence of maple leaves. *Tree Physiology*, 32(3), 346–354.

Gould, K.S., McKelvie, J. & Markham, K.R. (2002) Do anthocyanins function as antioxidants in leaves? Imaging of H_2O_2 in red and green leaves after mechanical injury. *Plant, Cell and Environment*, 25, 1261–1269.

Guiamét, J.J., Tyystjärvi, E., Tyystjärvi, T., John, I., Kairavuo, M., Pichersky, E. et al. (2002) Photoinhibition and loss of photosystem II reaction centre proteins during senescence of soybean leaves. Enhancement of photoinhibition by the 'stay-green' mutation cytG. *Physiologia Plantarum*, 115, 468–478.

Hernandez, I. & Van Breusegem, F. (2010) Opinion on the possible role of flavonoids as energy escape valves: novel tools for nature's Swiss army knife? *Plant Science*, 179(4), 297–301.

Hoch, W.A., Singsaas, E.L. & McCown, B.H. (2003) Resorption protection. Anthocyanins facilitate nutrient recovery in autumn by shielding leaves from potentially damaging light levels. *Plant Physiology*, 133, 1296–1305.

Huang, W., Chen, Q., Zhu, Y., Hu, F., Zhang, L., Ma, Z. et al. (2013) Arabidopsis thylakoid formation 1 is a critical regulator for dynamics of PSII-LHCII complexes in leaf senescence and excess light. *Molecular Plant*, 6, 1673–1691.

Hughes, N.M., Carpenter, K.S. & Cannon, J.G. (2013) Estimating contribution of anthocyanin pigments to osmotic adjustment during winter leaf reddening. *Journal of Plant Physiology*, 170, 230–233.

Hughes, N.M., George, C.O., Gumpman, C.B. & Neufeld, H.S. (2022) Coevolution and photoprotection as complementary hypotheses for autumn leaf reddening: a nutrient-centered perspective. *New Phytologist*, 233, 22–29.

Humbeck, K. & Krupinska, K. (2003) The abundance of minor chlorophyll a/b-binding proteins CP29 and LHCI of barley (*Hordeum vulgare* L.) during leaf senescence is controlled by light. *Journal of Experimental Botany*, 54, 375–383.

Hunt, R.E. & Daughtry, C.S.T. (2014) Chlorophyll meter calibrations for chlorophyll content using measured and simulated leaf transmittances. *Agronomy Journal*, 106, 931–939.

Ito, H., Saito, H., Fukui, M., Tanaka, A. & Arakawa, K. (2022) Poplar leaf abscission through induced chlorophyll breakdown by Mg-dechelatase. *Plant Science*, 324, 111444.

Järvi, S., Suorsa, M., Paakkarinen, V. & Aro, E.M. (2011) Optimized native gel systems for separation of thylakoid protein complexes: novel super- and mega-complexes. *Biochemical Journal*, 439, 207–214.

Ji, S.B., Yokoi, M., Saito, N. & Mao, L.S. (1992) Distribution of anthocyanins in *Aceraceae* leaves. *Biochemical Systematics and Ecology*, 20, 771–781.

Kale, R., Hebert, A.E., Frankel, L.K., Sallans, L., Bricker, T.M. & Pospíšil, P. (2017) Amino acid oxidation of the D1 and D2 proteins by oxygen radicals during photoinhibition of photosystem II. *Proceedings of the National Academy of Sciences of USA*, 114, 2988–2993.

Keskitalo, J., Bergquist, G., Gardeström, P. & Jansson, S. (2005) A cellular timetable of autumn senescence. *Plant Physiology*, 139(4), 1635–1648.

Kitao, M., Yazaki, K., Tobita, H., Agathokleous, E., Kishimoto, J., Takabayashi, A. et al. (2022) Exposure to strong irradiance exacerbates photoinhibition and suppresses N resorption during leaf senescence in shade-grown seedlings of fullmoon maple (*Acer japonicum*). *Frontiers in Plant Science*, 13, 1006413.

Kraj, W. & Zarek, M. (2021) Biochemical basis of altitude adaptation and antioxidant system activity during autumn leaf senescence in beech populations. *Forests*, 12, 529.

Kramer, D.M., Johnson, G., Kiirats, O. & Edwards, G.E. (2004) New flux parameters for the determination of QA redox state and excitation fluxes. *Photosynthesis Research*, 79, 209–218.

Krieger-Liszkay, A., Krupinska, K. & Shimakawa, G. (2019) The impact of photosynthesis on initiation of leaf senescence. *Physiologia Plantarum*, 166, 148–164.

Krieger-Liszkay, A., Trösch, M. & Krupinska, K. (2015) Generation of reactive oxygen species in thylakoids from senescing flag leaves of the barley varieties Lomerit and Carina. *Planta*, 241, 1497–1508.

Krupinska, K., Mulisch, M., Hollmann, J., Tokarz, K., Zschiesche, W., Kage, H. et al. (2012) An alternative strategy of dismantling of the chloroplasts during leaf senescence observed in a high-yield variety of barley. *Physiologia Plantarum*, 144, 189–200.

Kuai, B., Chen, J. & Hörtensteiner, S. (2018) The biochemistry and molecular biology of chlorophyll breakdown. *Journal of Experimental Botany*, 69, 751–767.

Kytridis, V.P. & Manetas, Y. (2006) Mesophyll versus epidermal anthocyanins as potential in vivo antioxidants: evidence linking the putative antioxidant role to the proximity of oxy-radical source. *Journal of Experimental Botany*, 57(10), 2203–2210.

Landi, M., Agati, G., Fini, A., Guidi, L., Sebastiani, F. & Tattini, M. (2021) Unveiling the shade nature of cyanic leaves: a view from the "blue absorbing side" of anthocyanins. *Plant, Cell & Environment*, 44(4), 1119–1129.

Lee, D.W., O'Keefe, J., Holbrook, N.M. & Field, T.S. (2003) Pigment dynamics and autumn leaf senescence in a New England deciduous forest, eastern USA. *Ecological Research*, 18, 677–694.

Lepeduš, H., Jurković, V., Štolf, I., Ćurković-Peric, M., Fulgosi, H. & Cesar, V. (2010) Changes in photosystem II photochemistry in senescing maple leaves. *Croatica Chemica Acta*, 83(4), 379–386.

Lepeduš, H., Štolfa, I., Radić, S., Ćurković Perica, M., Pevalek-Kozlina, B. & Cesar, V. (2008) Photosynthetic electron transport and superoxide dismutase activity during natural senescence of maple leaves. *Croatica Chemica Acta*, 81(1), 97–103.

Lev-Yadun, S. (2022) The phenomenon of red and yellow autumn leaves: hypotheses, agreements and disagreements. *Journal of Evolutionary Biology*, 35, 1245–1282.

Lihavainen, J., Edlund, E., Björkén, L., Bag, P., Robinson, K.M. & Jansson, S. (2021) Stem girdling affects the onset of autumn senescence in aspen in interaction with metabolic signals. *Physiologia Plantarum*, 172, 201–217.

Lo Piccolo, E., Landi, M., Pellegrini, E., Agati, G., Giordano, C., Giordani, T. et al. (2018) Multiple consequences induced by epidermally-located anthocyanins in young, mature and senescent leaves of *Prunus*. *Frontiers in Plant Science*, 9, 917.

Matile, P., Ginsburg, S., Schellenberg, M. & Thomas, H. (1988) Catabolites of chlorophyll in senescing barley leaves are localized in the vacuoles of mesophyll cells. *Proceedings of the National Academy of Sciences of USA*, 85, 9529–9532.

Mattila, H., Mishra, S., Tyystjärvi, T. & Tyystjärvi, E. (2023) Singlet oxygen production by photosystem II is caused by misses of the oxygen evolving complex. *New Phytologist*, 237, 113–125.

Mattila, H., Sotoudehnia, P., Kuuslampi, T., Stracke, R., Mishra, K.B. & Tyystjärvi, E. (2021) Singlet oxygen, flavonols and photoinhibition in green and senescing silver birch leaves. *Trees-Structure and Function*, 35, 1267–1282.

Mattila, H. & Tyystjärvi, E. (2023) Red pigments in autumn leaves of Norway maple do not offer significant photoprotection but coincide with stress symptoms. *Tree Physiology*, 43, 751–768. Available from: https://doi.org/10.1093/treephys/tpad010

Mattila, H., Valev, D., Havurinne, V., Khorobrykh, S., Virtanen, O., Antinluoma, M. et al. (2018) Degradation of chlorophyll and synthesis of flavonols during autumn senescence—the story told by individual leaves. *Annals of Botany Plants*, 10(3), ply028.

Miersch, I., Heise, J., Zelmer, I. & Humbeck, K. (2000) Differential degradation of the photosynthetic apparatus during leaf senescence in barley (*Hordeum vulgare* L.). *Plant Biology*, 2, 618–623.

Millard, P. & Thomson, C.M. (1989) The effect of the autumn senescence of leaves on the internal cycling of nitrogen for the spring growth of apple trees. *Journal of Experimental Botany*, 40(11), 1285–1289.

Moy, A., Le, S. & Verhoeven, S. (2015) Different strategies for photoprotection during autumn senescence in maple and oak. *Physiologia Plantarum*, 155, 205–216.

Naing, A.H. & Kim, C.K. (2021) Abiotic stress-induced anthocyanins in plants: their role in tolerance to abiotic stresses. *Physiologia Plantarum*, 172, 1711–1723.

Nath, K., Phee, B.K., Jeong, S., Lee, S.Y., Tateno, Y., Allakhverdiev, S.I. et al. (2013) Age-dependent changes in the functions and compositions of photosynthetic complexes in the thylakoid membranes of *Arabidopsis thaliana*. *Photosynthesis Research*, 117, 547–556.

Nikiforou, C., Nikopoulos, D. & Manetas, Y. (2011) The winter-red-leaf syndrome in *Pistacia lentiscus*: evidence that the anthocyanic phenotype suffers from nitrogen deficiency, low carboxylation efficiency and high risk of photoinhibition. *Journal of Plant Physiology*, 168, 2184–2187.

Nishiyama, Y., Yamamoto, H., Allakhverdiev, S.I., Inaba, M., Yokota, A. & Murata, N. (2001) Oxidative stress inhibits the repair of photodamage to the photosynthetic machinery. *The EMBO Journal*, 20, 5587–5594.

Oxborough, K. & Baker, N.R. (1997) Resolving chlorophyll *a* fluorescence images of photosynthetic efficiency into photochemical and non-photochemical components—calculation of qP and Fv′/Fm′ without measuring Fo′. *Photosynthesis Research*, 54, 135–142.

Pena-Novas, I. & Archetti, M. (2021) Missing evidence for the photoprotection hypothesis of autumn colours. *New Phytologist*, 232(6), 2236–2237.

Pesaresi, P., Scharfenberg, M., Weigel, M., Granlund, I., Schröder, W.P., Finazzi, G. et al. (2009) Mutants, overexpressors, and interactors of arabidopsis plastocyanin isoforms: revised roles of plastocyanin in photosynthetic electron flow and thylakoid redox state. *Molecular Plant*, 2, 236–248.

Platt, T., Gallegos, C.L. & Harrison, W.G. (1980) Photoinhibition of photosynthesis in natural assemblages of marine phytoplankton. *Journal of Marine Research*, 38, 687–701.

Porra, R.J., Thompson, W.A. & Kriedemann, P.E. (1989) Determination of accurate extinction coefficients and simultaneous equations for assaying chlorophylls *a* and *b* extracted with four different solvents: verification of the concentration of chlorophyll standards by atomic absorption spectroscopy. *Biochimica et Biophysica Acta*, 975, 384–394.

Pospíšil, P. & Yamamoto, Y. (2017) Damage to photosystem II by lipid peroxidation products. *Biochimica et Biophysica Acta*, 1861, 457–466.

Rangel, M., Machado, O.L.T., da Cunha, M. & Jacinto, T. (2002) Accumulation of chloroplast-targeted lipoxygenase in passion fruit leaves in response to methyl jasmonate. *Phytochemistry*, 60, 619–625.

Rantala, M., Paakkarinen, V. & Aro, E.M. (2018) Analysis of thylakoid membrane protein complexes by blue native gel electrophoresis. *Journal of Visualized Experiments*, 139, 58369.

Renner, S.S. & Zohner, C.M. (2022) Trees growing in eastern North America experience higher autumn solar irradiation than their European relatives, but is nitrogen limitation another factor explaining anthocyanin-red autumn leaves? *Journal of Evolutionary Biology*, 35, 183–188.

Schöttler, M.A. & Tóth, S.Z. (2014) Photosynthetic complex stoichiometry dynamics in higher plants: environmental acclimation and photosynthetic flux control. *Frontiers in Plant Science*, 5, 188.

Shimakawa, G., Krieger-Liszkay, A. & Roach, T. (2022) ROS-derived lipid peroxidation is prevented in barley leaves during senescence. *Physiologia Plantarum*, 174, e13769.

Shimakawa, G., Roach, T. & Krieger-Liszkay, A. (2020) Changes in photosynthetic electron transport during leaf senescence in two barley varieties grown in contrasting growth regimes. *Plant and Cell Physiology*, 61, 1986–1994.

Shinopoulos, K.E. & Brudvig, G.W. (2012) Cytochrome b559 and cyclic electron transfer within photosystem II. *Biochimica et Biophysica Acta*, 1817, 66–75.

Sinkkonen, A. (2008) Red reveals branch die-back in Norway maple *Acer platanoides*. *Annals of Botany*, 102(3), 361–366.

Soubeyrand, E., Colombié, S., Beauvoit, B., Dai, Z., Cluzet, S., Hilbert, G. et al. (2018) Constraint-based modeling highlights cell energy, redox status and α-ketoglutarate availability as metabolic drivers for anthocyanin accumulation in grape cells under nitrogen limitation. *Frontiers in Plant Science*, 9, 421.

Springer, A., Kang, C.H., Rustgi, S., von Wettstein, D., Reinbothe, C., Pollmann, S. et al. (2015) Programmed chloroplast destruction during leaf senescence involves 13-lipoxygenase (13-LOX). *Proceedings of the National Academy of Sciences of USA*, 113(12), 3383–3388.

Tamary, E., Nevo, R., Naveh, L., Levin-Zaidman, S., Kiss, V., Savidor, A. et al. (2019) Chlorophyll catabolism precedes changes in chloroplast structure and proteome during leaf senescence. *Plant Direct*, 3(3), 1–18.

Tang, Y., Wen, X. & Lu, C. (2005) Differential changes in degradation of chlorophyll–protein complexes of photosystem I and photosystem II during flag leaf senescence of rice. *Plant Physiology and Biochemistry*, 43, 193–201.

Taulavuori, E., Tahkokorpi, M., Laine, K. & Taulavuori, K. (2010) Drought tolerance of juvenile and mature leaves of a deciduous dwarf shrub *Vaccinium myrtillus* L. in a boreal environment. *Protoplasma*, 241, 19–27.

Theis, J. & Schroda, M. (2016) Revisiting the photosystem II repair cycle. *Plant Signaling & Behavior*, 11(9), e1218587.

Tyystjärvi, E. (2013) Photoinhibition of photosystem II. *International Review of Cell and Molecular Biology*, 300, 243–303.

Tyystjärvi, E. & Aro, E.M. (1996) The rate constant of photoinhibition, measured in lincomycin-treated leaves, is directly proportional to light intensity. *Proceedings of the National Academy of Sciences of USA*, 93, 2213–2218.

van den Berg, A.K. & Perkins, T.D. (2007) Contribution of anthocyanins to the antioxidant capacity of juvenile and senescing sugar maple (*Acer saccharum*) leaves. *Functional Plant Biology*, 34(8), 714–719.

van Heerwaarden, L.M., Toet, S. & Aerts, R. (2003) Current measures of nutrient resorption efficiency lead to a substantial underestimation of real resorption efficiency: facts and solutions. *Oikos*, 101, 664–669.

Wang, P. & Grimm, B. (2021) Connecting chlorophyll metabolism with accumulation of the photosynthetic apparatus. *Trends in Plant Science*, 26, 484–495.

Wang, X., Chen, Y., Liu, F., Zhao, R., Quan, X. & Wang, C. (2020) Nutrient resorption estimation compromised by leaf mass loss and area shrinkage: variations and solutions. *Forest Ecology and Management*, 472, 118232.

Wang, Y., Zhang, J., Yu, J., Jiang, X., Sun, L., Wu, M. et al. (2014) Photosynthetic changes of flag leaves during senescence stage in super high-yield hybrid rice LYPJ grown in field condition. *Plant Physiology and Biochemistry*, 82, 194–201.

Wellburn, A.R. (1994) The spectral determination of chlorophylls a and b, as well as total carotenoids, using various solvents with spectrophotometers of different resolution. *Journal of Plant Physiology*, 144, 307–313.

Wolf, F.T. (1956) Changes in chlorophyll-*a* and chlorophyll-*b* in autumn leaves. *American Journal of Botany*, 43, 714–718.

Yadav, D.K. & Pospíšil, P. (2012) Evidence on the formation of singlet oxygen in the donor side photoinhibition of photosystem II: EPR spin-trapping study. *PLoS One*, 7(9), e45883.

Yutthanasirikul, R., Nagano, T., Jimbo, H., Hihara, Y., Kanamori, T., Ueda, T. et al. (2016) Oxidation of a cysteine residue in elongation factor EF-Tu reversibly inhibits translation in the cyanobacterium *Synechocystis* sp. PCC 6803. *The Journal of Biological Chemistry*, 291, 5860–5870.

Zhu, H. & Wild, A. (1995) Changes in the content of chlorophyll and redox components of the thylakoid membrane during development and senescence of beech (*Fagus sylvatica*) leaves. *Zeitschrift für Naturforschung. Section C*, 50, 69–76.

SUPPORTING INFORMATION

Additional supporting information can be found online in the Supporting Information section at the end of this article.

How to cite this article: Rantala, M., Mulo, P., Tyystjärvi, E. & Mattila, H. (2023) Biophysical and molecular characteristics of senescing leaves of two Norway maple varieties differing in anthocyanin content. *Physiologia Plantarum*, 175(5), e13999. Available from: https://doi.org/10.1111/ppl.13999